J Mater Sci: Mater Med (2008) 19:1881–1889
DOI 10.1007/s10856-007-3247-7

Effect of treated filler loading on the photopolymerization inhibition and shrinkage of a dimethacrylate matrix

T. G. Nunes · S. G. Pereira · S. Kalachandra

Received: 24 November 2006 / Accepted: 26 July 2007 / Published online: 4 October 2007

Abstract This study shows how treated filler loading influences the photopolymerization of a dimethacrylate comonomer mixture, regarding, in particular, shrinkage and inhibition under atmospheric oxygen, present in oral environment. Bis-GMA/TEGDMA (75/25 wt.%) resins were loaded with hybrid filler (Ba aluminosilicate glass and pyrogenic silica), treated with γ-methacryloxy(propyl)trimethoxysilane, at 0–50 wt.% and light cured over a total of 30 s (45 mW/cm^2). Degree of double-bond conversion (DC), obtained using FTIR, decreased with filler content. ^{1}H MAS spectra (293–340 K) and STRAFI images (293 K) were obtained as a function of irradiation time and filler concentration. ^{1}H signals of unreacted methacrylate groups were more intense for higher loaded resins and resonances from –$CH_2SiO_2(OH)$ (T^2) and –CH_2SiO_3– (T^3) units, also observed by ^{29}Si NMR, were resolved and suggest the presence of T^2–resin bonds. 1D images show a reduction on polymerization contraction and reaction inhibition at the composite resin surface with filler loading. 2D resin images present a highly mobile surface layer, hence with lower DC.

T. G. Nunes (✉) · S. G. Pereira
Departamento de Engenharia de Materiais/IST, Univ. Técnica de Lisboa, Av.Rovisco Pais 1, Lisboa 1049-001, Portugal
e-mail: Teresa.Nunes@ist.utl.pt

S. Kalachandra
Dental Research Center, University of North Carolina COSD, Chapel Hill, NC, USA

1 Introduction

The major components of dental composite resins (CR) are the polymer matrix and the filler, which is usually a particulate glass pre-treated with a silane, for example γ-methacryloxy(propyl)trimethoxysilane (SIL) (Fig. 1c), in order to minimize particle-particle interaction, which imposes a filler loading constraint, and to promote resin-filler coupling. Previous works showed that filler particles do exert an important mechanical reinforcement [1] and an increase in the hydrophobic character [2]. Moreover, the addition of filler is also a mean of reducing polymerization shrinkage [3].

Silica and alumina surfaces chemically modified by reaction with SIL were characterized by infrared spectroscopy, using the diffuse reflection technique (DRIFT), and solid-state magic angle spinning (MAS) nuclear magnetic resonance (NMR) spectroscopy; the formation of chemical bonds involving the silane methoxyl groups and silanols from the silica surface was demonstrated and it was found that geminal silanols were more reactive than free silanols [4].

CRs are generally visible-light cured, in the presence of a photoinitiator system, reaching a maximum degree of conversion (DC) of about 75%. The reaction is highly anisotropic, mainly due to light-absorption and -scattering by filler particles and to the oxygen inhibitor effect, processes that affect DC [5]. Accordingly, at the end of the irradiation period, a considerable amount of mobile monomers and non-photopolymerized methacrylate groups remain in the rigid polymeric matrix and ensuing release of unreacted monomers is favoured in aqueous environment. The decrease of physical/mechanical properties, is also related to a hydrolytic breakdown of the bond between silane and filler particles, filler and matrix or hydrolytic

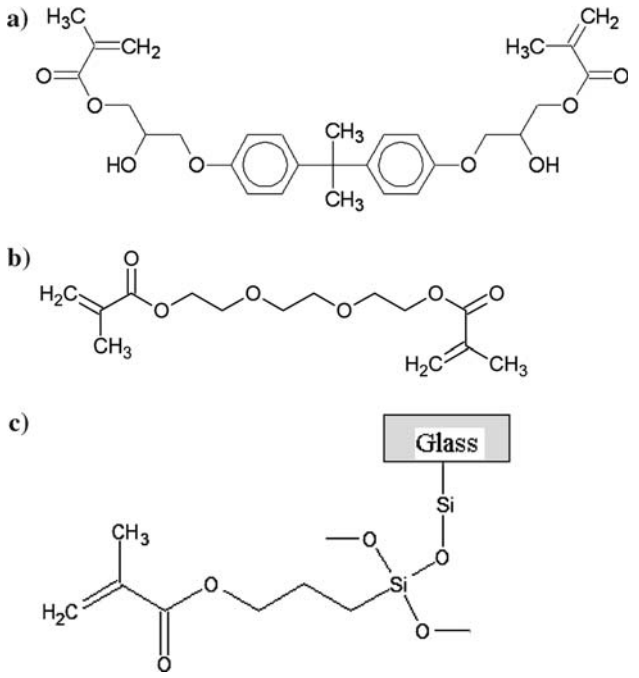

Fig. 1 Chemical structure of: (**a**) Bis-GMA, (**b**) TEGDMA and (**c**) γ-methacryloxypropyltrimethoxysilane

degradation of the fillers [5]. In fact, except when kinetically stabilized, hydroxides of silicon are unstable and readily self-condense through elimination of water molecules to yield Si–O–Si siloxane linkages.

Overall, the performance of CR in oral environment is highly dependent on DC; however, the influence of the filler in the resin methacrylate double bond conversion remains a controversial subject. For example, opposite conclusions were published in [6] and [7]. Zirconia/silica fillers (average particle size 0.6 μm) were silanized using SIL in order to obtain silane-treated fillers with 4–20 wt.% silane and the corresponding methacrylate unsaturation were obtained by DRIFT. Bis-GMA (2,2-bis-4–(2-hydroxy-3-methacryloyl-oxypropoxy) phenyl propane) (Fig. 1a) /TEGDMA (triethylene glycol dimethacrylate) (Fig. 1b), (50/50 wt.%) resins were filler loaded to 72% either with untreated filler or with silane-treated fillers with 4–20 wt.% silane and after a light-irradiation period of 30 s (the intensity of light was not mentioned), DC was obtained by FTIR, without or with correcting for the presence of C=C bonds on silane molecules, which usually leads to underestimated DC; similar corrected conversions (65.1 ± 0.8%) were obtained for each of the paste formulation and the increase of filler content (8% silane-treated) has led to *progressively lower DC with filler loading* of the silane-treated pastes [6]. The influence of filler loading in Bis-GMA/TEGDMA (65/35 wt.%) resins was recently reported [7]; silanized barium aluminium glass fillers (silanized with 1.5 wt.% SIL and with an average particle size of 3.4 μm) were used and the pastes were cured over 40 s at 550 mW/cm^2; it was concluded that *the filler fraction did not affect DC*. Both published works [6, 7] have in common the fact that the influence of oxygen, a radical scavenger, was not taken into account; according to [7], the different behaviour of composite resins could be explained by the use of fillers with different specific surface area, which was much higher in [6].

In this study, we have also used a Bis-GMA/TEGDMA monomer matrix in order to assess the role of filler loading in DC, polymerization shrinkage and molecular dynamics in the presence of oxygen from the atmosphere, condition that mimics in vivo environment. For this purpose, were employed ^{1}H stray-field MRI and multinuclear solid-state MAS NMR (non-invasive and non-destructive techniques) to map and to assign more mobile domains in CR as a function of filler loading and to evaluate the polymerization shrinkage and anisotropy, DC was obtained by FTIR. The treated filler was also characterized by solid-state NMR and, to our knowledge, only grafting of the organic silane SIL onto silica and alumina nanoparticles have been investigated using this technique [4].

2 Materials and methods

2.1 Materials

A homogeneous comonomer mixture of 75 wt.% Bis-GMA (Polysciences Inc.) and 25 wt.% TEGDMA (Aldrich Chemical Co., Milwaukee, WI, USA) was prepared and a photoinitiator system was added (1/1 mol%): camphorquinone (CQ, Aldrich Chemical Co., Milwaukee, WI, USA) and *N*,*N*-dimethyl-*p*-toluidine (DMPT, Aldrich Chemical Co., Milwaukee, WI, USA). CQ was sublimed at 140 °C under reduced pressure before using and DMPT was used as received. Subsequently, this solution was used to prepare five CR with 0, 10, 25, 35 and 50 wt.% filler loading; the viscosity of the unfilled resin was about 2 Pa s [8]. The filler was a silanated hybrid filler (Herculite, Kerr, USA) with an average particle size of 0.7 μm. The filler particles were from Ba aluminosilicate glasses and pyrogenic silica treated with SIL (Fig. 1c; the presence of CH_3–O– occurs only if hydrolysis is incomplete). Photopolymerized resins and CR were obtained following visible light irradiation (maximum at 470 nm, Optilux 401, Demetron Research Corp., Danbury, CT, USA) while keeping the light-guide at a distance of 3 cm from the sample surface; hence, light intensity was about 45 mW/cm^2, that is about a factor of 10 below the value recommended to clinicians. The light-intensity used here was selected in order to achieve lower final DC and thus enabling spatial curing anisotropy to be enhanced.

2.2 Methods

2.2.1 NMR spectroscopy

NMR solid state spectroscopic studies were performed using a Bruker MSL 300 P spectrometer operating at 300.13, 75.47 and 59.60 MHz for ^{1}H, ^{13}C and ^{29}Si observations, respectively. ^{1}H MAS spectra were obtained from the filler and from CR photopolymerized over the indicated irradiation time (10 s or 10 + 20 s), in the temperature range 293–340 K. Zirconia rotors with 16 mm height and 7 or 4 mm outer diameter (also the dimensions of the specimens), were used when selecting 4 or 7 kHz MAS rate, respectively. The spectra were acquired using a spin-echo RF pulse sequence ($90°_{y}$-τ-$180°_{x}$-τ-signal acquisition), with a long delay τ (800 μs); this sequence acts as a simple spin filter allowing proton signals from mobile parts of the samples to be enhanced. The pulse duration corresponding to a 90° magnetisation tip angle ($t_{90°}$) was 5 μs. The standard Cross Polarization/MAS (CP/MAS) technique (with proton decoupling) was used to observe ^{13}C ($t_{90°}$ 5.1 μs, contact time 1 or 10 ms, relaxation delay 3 s, MAS 4 kHz) and ^{29}Si resonances (contact time 5 ms, relaxation delay 5 s, number of scans 14000, MAS at about 4 kHz) on different samples (filler, resins or CR, as specified along the text). As external references for ^{1}H, ^{29}Si and ^{13}C resonances were used TMS (0 ppm) and glycine (^{13}CO group at 176.1 ppm), respectively.

2.2.2 ^{1}H stray-field MRI

One-dimensional ^{1}H STRAFI images, projections along an axis, were acquired from liquid and cured CR using a Bruker MSL 300P spectrometer, under the static magnetic field gradient of 37.5 T/m generated near the edges of the 89 mm superconducting coil. A dedicated Bruker STRAFI probe-head was tuned to 123.4 MHz, which gives ^{1}H resonance at 2.9T; this field strength was obtained just outside the bore of the magnet. Each liquid resin was introduced in a cylindrical glass vial (10 mm height and 5 mm inner diameter) filled up to about 4 mm height and irradiated outside the magnet over 10 s and 10 + 20 s. The experimental set-up and the protocol, which was followed were previously described [9]. One-dimensional images (profiles) were acquired along the container axis after each irradiation period. A reference signal for the intensities was obtained from a disc about 0.5 mm thick, made of commercial plastic, which was placed under the glass vials. The photopolymerization was carried out at room temperature (about 294 K). The magnetization was recorded as multiple 16 spin-echo trains (see [10] for details) with echo time (TE) 35 μs and $t_{90°}$ 10 μs. The linear resolution was about 50 μm. Each echo decay, which is the magnetization decay of one slice, is mainly governed by the spin–spin relaxation time (T_2); accordingly, each data slice in the projections was obtained either using all the 16 echoes or just the last eight echoes, in each echo train, in order to enhance the domains more mobile in the kHz frequency range. Thus, each data point in the profiles is the result of the summation of all the echoes (16) or just of the last eight echoes in each echo train. 2D data was acquired and 2D images were reconstructed either using all the echoes or just the last eight echoes in each echo train. The resolution of a pixel was: 0.1×0.1 mm^2. Data were acquired at the probe-head temperature ($\sim$293 K).

The final volumetric polymerization contraction (VPC, in %) was determined for the unfilled resin and for the resin 50 wt.% filler loaded, according to a method previously described [11], as: [Σ (magnetization of each slice of the resin, MM) – Σ (magnetization of each slice of the cured resin, MP) × 100]/Σ (MM). The highest intensity of MP was used as a reference for the intensity normalization of the magnetization MM and MP slices.

2.2.3 FTIR spectroscopy

The degree of double-bond conversion of CR was obtained by FTIR spectroscopy. Transmission FTIR spectra were obtained using a Perkin–Elmer spectrometer (Model 1710). The spectra of monomers and comonomer mixture were recorded on one scan over the range 650–4000 cm^{-1} using a drop of the liquid smeared between NaCl plates. For the observation of photopolymerized CR, about 2 mg of powdered solid was pressed into a pellet with approximately 70 mg of KBr. Spectra were obtained with 10 scans over the range 650–4000 cm^{-1}. The FTIR method to determine degree of double-bond conversion (DC, in %) in dental materials was already discussed in detail [12, 13]. The peaks used in the analysis were the methacrylate C=C absorbance at 1640 – 1635 cm^{-1} and the aromatic C=C absorbance at 1610 – 1605 cm^{-1}. The aromatic peak originates from the aromatic rings in the Bis-GMA molecule, the amount of which remains unchanged during the polymerization. DC was obtained by comparing the ratio of the methacrylate and the aromatic absorbances before and after polymerization according to:

$$DC = \left[1 - \frac{(A_{meth}/A_{arom})polymer}{(A_{meth}/A_{arom})monomer}\right] \times 100$$

where A_{meth} and A_{arom} are the absorbances of the methacrylate and aromatic bands, respectively. The peak heights were used for this determination.

3 Results and discussion

NMR is often used for materials characterization as it provides structural and conformational information at the atomic level; in addition, relaxation rates allow probing molecular dynamics over a wide range of time scales. Mechanical properties of CR, such as toughness, depend strongly on polymer main chain mobility in the kHz frequency range, which is influenced by the filler. Nevertheless, NMR has not been extensively applied to polymer surface and interface studies because of low sensitivity and difficulty in separating surface layers from the bulk. However, proton NMR has the highest sensitivity, allowing the study of several materials with poorer surface area [13], including the interfacial surface chemistry in dental composites (treated filler-resin matrix) studied here and complemented with ^{13}C and ^{29}Si NMR data. ^{1}H STRAFI-MRI was used to observe profiles and 2D images of resins and CR.

3.1 NMR spectroscopy

Multinuclear magnetic resonance studies were performed on the treated filler, CR (^{29}Si, ^{13}C, ^{1}H) and resin (^{13}C, ^{1}H) in order to characterize the samples aiming, in particular, to distinguish covalently- and physically-adsorbed filler particles.

3.1.1 ^{29}Si CP/MAS NMR spectroscopy

^{29}Si NMR is a very powerful tool to characterize silicate materials. It can provide evidence for the presence of chemical bonds between silanol groups from glass surface and the coupling agent and for the reactivity of the different silanol species. ^{29}Si resonances of the grafted silyl groups are shifted to higher magnetic field when siloxane bonds are created between these groups and silica and this displacement increases with the number n of siloxanes, T^n, that is from T^1 to T^3 units.

^{29}Si CP/MAS spectrum of the particulate filler is displayed on Fig. 2. The chemical shifts of ^{29}Si CP/MAS NMR signals of silica silicons and grafted trifunctional silanes may be found elsewhere [4]. In particular, peaks observed in the range from –50 to –80 ppm are assigned to different surface compounds of trifunctional silanes in the chemically modified silica surface. At least three signals are observed in the spectrum shown in Fig. 2; the major signal, which is broad because glasses present a distribution of electronic environments, is observed at –98 ppm, with a full width at half maximum (FWHM) of 1100 Hz, can be assigned, for example, either to silicon tetrahedra with one Al in the second coordination sphere (Si(1Al)) or to $–O_3SiOH$ (Q^3) units, and the two less intense peaks (at –58 ppm and –67 ppm with FWHM about 200 Hz) are from the grafted organosilanes and are assigned to di- (T^2) and tri- (T^3) fold Si–O-linked silicon atoms, respectively [14,15]: $–CH_2SiO_2(OH)$ (T^2) and $–CH_2SiO_3–$ (T^3). Hence, judging from ^{29}Si NMR data, the concentration of $–O_4Si$ (Q^4) units was very low (with resonance in the range –110 to –120 ppm) and the silane was mostly in the tridentate form and no monodentate bonding of silanes was observed, that is T^1 species, result that agrees well with previously reported characterization on silane-modified silica surfaces [15]. There was no indication for the presence of free SIL (the corresponding resonance is at –43.1 ppm). Typical acrylate formulations mentioned in [15] contained about 20–40 wt.% modified silica, that is, about twice more than the grafted filler used here, as can be concluded by comparing the relative intensities of ^{29}Si major resonances assigned to Q^3 and T^3 units in Fig. 2 with those in Fig. 3b in [15]. Accordingly, a less efficient H–Si cross polarization explains the poorer ^{29}Si signal/noise ratio of the spectrum shown here. SIL concentration of the grafted filler in CR was too low and, thus, no evidence could be obtained by ^{29}Si NMR for the polymerization of the silane functional group. It was already reported on that ^{29}Si resonances didn't show to be affected by interaction with polymeric matrix with [15].

3.1.2 ^{13}C CP/MAS NMR spectroscopy

Additional information about the particulate filler and cured samples was obtained from ^{13}C solid state NMR. Figure 3 shows ^{13}C CP/MAS (4.2 kHz) spectra that were

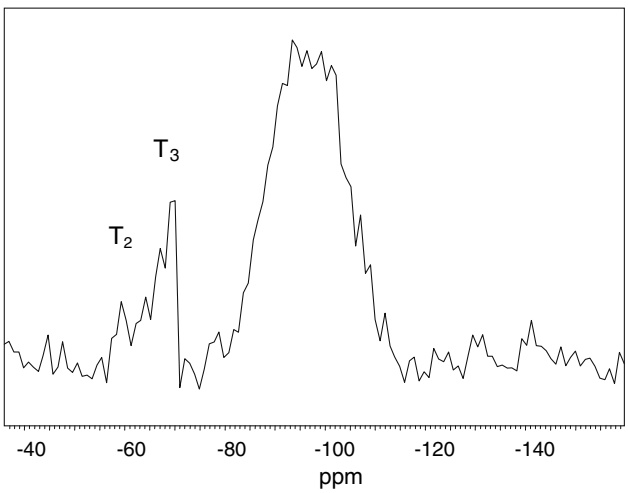

Fig. 2 ^{29}Si CP/MAS (4 kHz) spectra obtained at about 293 K from the treated filler

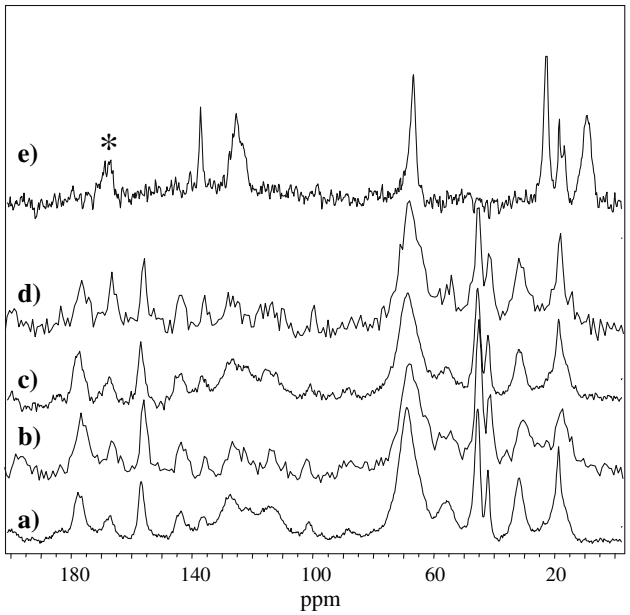

Fig. 3 ^{13}C CP/MAS (4.2 kHz) spectra of: (**a**) and (**b**) resin, obtained with a contact time (CT) of 1 and 10 ms, respectively, (**c**) and (**d**) composite resin with 50 wt.% of filler, obtained with CT of 1 or 10 ms, respectively, and (**e**) treated filler, recorded with CT of 1 ms. Light-curing was over 10 + 20 s (45 mW/cm^2) for the resin and composite resin. All the spectra were observed at about 293 K. Carbonyl signals from unreacted methacrylate groups are assigned with an asterisk

obtained from treated filler, cured CR (50 wt.% filler) and cured resin; light-curing was over 10 + 20 s (45 mW/cm^2), for the resin and CR, and contact times (CT) of 1 and 10 ms were selected for the acquisition of spectra 3a, c and 3b, d, respectively. Figure 3e shows the spectrum of treated filler recorded with a CT of 1 ms. It is well known that, for carbons with identical multiplicity like quaternary carbonyl carbons in reacted (R) and unreacted methacrylate (UR) moieties, longer CT will favour signals from UR, with higher mobility. Hence, these spectra can provide a rough estimate of DC, which is directly obtained by integration of the signals assigned to C=O in R (CO_R at δ 176.5 ppm) and UR (CO_{UR} at δ 166.5 ppm): DC (mol%) = 100 × [CO_R/(CO_R + CO_{UR})]. Using this procedure, the following DC were obtained: a) 72 ± 2 mol % for the resin (a similar value was obtained from 3a and 3b spectra, which were acquired with different CT), b) 70 and 54 mol% for the composite resin, obtained from the spectra run with 1 and 10 ms CT, respectively. This effect is in agreement with higher molecular mobility in cured CR as compared with cured resin, hence with lower DC in loaded resins, result that agrees well with FTIR data (Table 1). It must be pointed out here that determination of extent of reaction in dimethacrylates by solid-state ^{13}C MAS (with and without CP) spectroscopy was already compared with FTIR information [16] and, more recently, it was shown that the presence of silanized glass fillers can lead to underestimated DC, when only transmission FTIR is used [6].

The chemical shifts obtained from SIL (in $CDCl_3$) [17] and grafted filler are shown in Table 2. Figure 3e shows broader signals for *C*O, vinylic *C*H_2 and CH_2–*C*H_2–Si groups and this is consistent with a distribution of electronic shielding, hence with different structural localization of the indicated carbon atoms. In SIL, the γ-shielding effect of each CH_3 on α*C*H_2 is about –2.5 ppm [18] and α*C*H_2 resonance is at 5.5 ppm. Accordingly, observation of α*C*H_2 signal at 9.2 ppm for the filler is already an indication of hydrolysis, with substitution of CH_3 by H. Moreover, hydrolysis reaction was complete because, otherwise, a signal from methoxyl groups would appear at 50.6 ppm in the spectrum of the silanized filler (Fig. 3e). In general, two routes may be followed for the silanization of glasses: (a) Silanols are obtained as hydrolysis products of the alkoxy substituents of SIL and subsequently react with OH groups of silica in the glass to build up surfaces siloxane units; (b) Methoxyl groups of SIL can form a chemical bond with OH groups of silica in the glass to build up surfaces siloxane units. In both routes, silanols can also just interconnect and condense by reacting with other silanol groups, but these products can be easily removed [14]. The treated filler used in the present work was most probably obtained according to route (a) which allows controlling hydrolysis before glass grafting thus favouring a complete reaction, as probed here by NMR spectroscopy.

^{13}C spectra of cured CR are dominated by signals from the polymer matrix (Fig. 3c and d); the assignment of Bis-GMA and TEGDMA carbon signals was previously reported [19]. These spectra show an important contribution of resonances from unreacted methacrylate groups (for example *C*O appear at 166.5 ppm), which are more intense for higher loaded CR; incomplete polymerization was confirmed by FTIR (DC data, which are shown in Table 1, were 32.0 ± 0.7 and 49.6 ± 0.9 mol% for 50 wt.% filler loaded and unloaded resin, respectively). The resonances from the grafted silane were not assigned in the ^{13}C spectra

Table 1 Degree of double-bond conversion (DC) obtained from FTIR measurements for the resin and composite resins with the indicated resin/filler ratio

Resin/Filler (wt %)	100/0	90/10	75/25	65/35	50/50
DC (mol %)	49.6 ± 0.9	37.3 ± 0.6	36.1 ± 0.1	33.6 ± 0.2	32.0 ± 0.7

Table 2 ^{13}C and ^{1}H chemical shifts (ppm) of SIL (R=CH_3) in $CDCL_3$ obtained from [17] and of silanized glass particles obtained here from CP/MAS and MAS spectra, respectively

Compound	Spectrum	CH_2	= C	– (CH_3)	(CO)	– O – CH_2	– CH_2	– CH_2	– Si – $(OR)_3$
SIL	^{13}C	126.1	136.7	18.3	167.4	66.6	22.3	5.5	50.6
	^{1}H	6.10; 5.54		1.94		4.12	1.80	0.70	3.58
Grafted glass	$^{13}C^{a}$	125.3	137.1	18.4	167.5	66.6	22.7	9.2	–
	^{1}H	6.0; 5.5		1.8		4.3		1; 0.7	3.7

[a] the resonance at 16.7 ppm was not assigned

obtained from CR due to overlapping with resin signals; hence, no evidence could be obtained for the presence of silane methacrylic groups chemically bond to the resin.

3.1.3 *^{1}H NMR spectroscopy*

^{1}H MAS spectra of the silanized filler obtained in the temperature range 293–340 K are shown in Fig. 4a. Only qualitative results can be extracted from these spectra

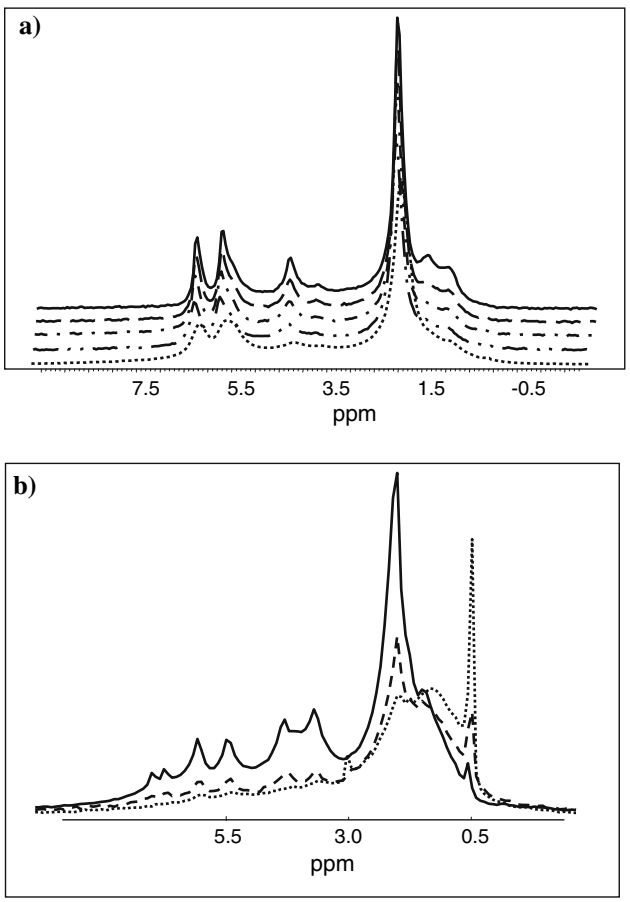

Fig. 4 ^{1}H MAS spectra at 7 kHz of: (**a**) treated filler, obtained at 293, 310, 318, 329 and 340 K (from the bottom to the top); (**b**) composite resin containing 50 wt.% filler cured over 10 + 20 s (45 mW/cm^2) obtained at 293 (*dot line*), 310 (*dash line*) and 340 K (*straight line*)

because contributions from very broad resonances were not recorded due to the use of a spin–spin relaxation filter for data acquisition. Chemical shifts of the grafted filler are shown in Table 2 and can be compared with the corresponding data obtained from SIL (in $CDCL_3$) [17]; signals at about 6 and 5.5 ppm are assigned to the methylenic protons in methacrylate moieties, respectively *cis* and *trans* to the carbonyl group, and the signal at 3.7 ppm is tentatively assigned to –OH groups, in $–CH_2SiO_2(OH)$ (T^2) units. At 340 K, another two signals appear at about 1 and 0.7 ppm and are assigned to αCH_2 to the silicon atom in T^2 and T^3 ($–CH_2SiO_3–$) units, respectively; at our knowledge, this is the first time that both signals were well resolved. This assignment is supported by the fact that, for methylene groups, the chemical deshielding increment to be added to the base value 1.37 ppm due to αSi(OR)(OR)OR is –0.75 ppm, yielding a predicted value of 0.62 ppm for the chemical shift [20]; on the other hand, in a compound with $Si[OSi(CH_3)_3]_3$ instead of $Si[OCH_3]_3$, which is present in SIL, hence with groups with an electronic shielding more similar to T^3 units, the chemical shift of αCH_2 is about 0.5 ppm, that is upfield shifted comparatively with SIL data (Table 2) [17]. There is a good correspondence between the chemical shifts of hydrogen nuclei in the grafted structures and those of SIL, as it was already pointed out [4]. However, the resonances from the solid are not all shifted downfield in comparison with the corresponding ^{1}H chemical shifts of SIL in $CDCl_3$ (Table 2), as published before [4]. ^{1}H MAS spectra were also obtained from CR cured over 10 + 20 s. Figure 4b shows ^{1}H spectra of CR containing 50 wt.% filler that were obtained under a MAS rate of 7 kHz at 293, 310 and 340 K, respectively. It is observed a line narrowing effect with temperature, which is related to longer spin–spin relaxation time (T_2, which probes mobility in the kHz range) and is due to molecular mobility being favoured at higher temperature, specially near the T_g of the resin, which is about 338 K [11], and involving then not only mobile groups but also polymeric chains. In the spectrum recorded at 293 K, the signal with the highest intensity is also the narrowest and appears at 0.5 ppm. The relative intensity of this resonance decreases strongly with temperature and this fact is explained because, at higher temperatures, the mobility of other

chemical groups in the resin and silanized filler is favoured and, accordingly, T_2 also increases thus enabling the observation of a higher signal contribution from those groups; hence, this resonance is tentatively assigned to –CH_2–Si groups in T^3 units of physically adsorbed treated filler particles, not involved in exchange processes, in which case the corresponding signal would be also shifted at higher temperature. Only a very broad signal, centred at about 1.1 ppm in the spectra run at 293 K, is identified in the frequency range corresponding to –CH_2–Si groups in T^2 units This fact can be explained by the presence of –CH_2–Si groups with a distribution of electronic environments, most possibly due to cross-linkages involving methacrylic units of the silane and the monomers; hydrogen bonding of (–CH_2SiO_2(OH)) can not be discarded as well. Hence, these data point to the presence of silane-resin chemical interaction, which appears to involve T^2 units predominantly. Figure 5 allows the comparison of ^{1}H MAS spectra of unfilled and CR containing 50 wt.% of filler and cured only over 10 s, which is less than the irradiation time selected for the previous samples, obtained at 340 K under a MAS rate of 4.3 kHz. Overall, both spectra display narrow signals, particularly from unreacted methacrylate groups; improved signal to noise ratio and resolution are noticed in the case of the loaded resin. This observation is in agreement with higher molecular mobility, which could be explained by a lower degree of double bond conversion in the presence of the filler and/or by the presence of unreacted methacrylate groups from the silane. CH_3 peak displays a shoulder at low frequency, which is assigned to methyl groups in the bisphenol Bis-GMA moiety, superimposed to βCH_2 to the silicon atom in T^2 and T^3 units. New signals were obtained in the CR spectrum, which appear at about 0.7 and 0.5 ppm and are assigned to –CH_2–Si groups in T^2 and T^3 units, respectively, previously identified at about 1 and 0.7 ppm in the spectrum of the silane treated filler (Fig. 4a). Clearly, these silane resonances, appear better resolved and shifted to high field in the presence of the resin (Fig. 5b); this observation is in agreement with higher mobility of the silane, effect most probably enhanced in the case of T^2 units due to a less extent of chemical interaction with the copolymer cured over insufficient time (10 s).

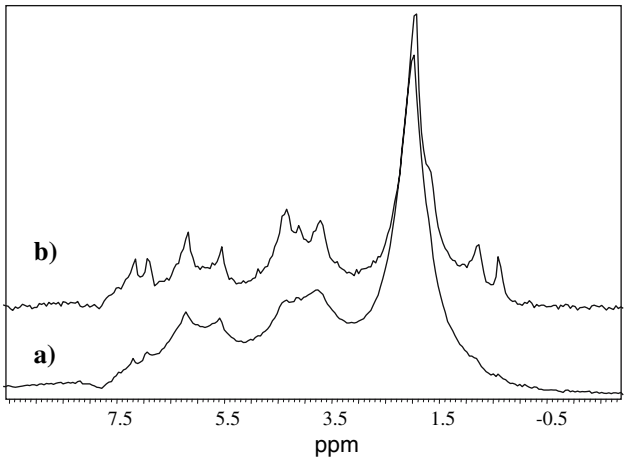

Fig. 5 ^{1}H MAS spectra obtained at 340 K with a spinning rate of 4.3 kHz from the following cured samples (10 s, 45 mW/cm^2): (**a**) unfilled resin and (**b**) composite resin containing 50 wt.% of filler

3.2 ^{1}H stray-field MRI

^{1}H STRAFI-MRI was used in order to acquire proton density maps from cured samples, which are also spatially-resolved images of molecular dynamics; in fact, the signal intensity depends on hydrogen concentration but is strongly weighted by relaxation processes, mainly those governed by spin–spin relaxation which are controlled by molecular mobility in the kHz frequency range, as it was already pointed out. Hence, the last echoes in each echo train are mostly from mobile molecules like monomers and oligomers, with longer T_2 (see the experimental section for details); an improved contrast may be achieved by using only these echoes to reconstruct the images because molecular mobility differences are then enhanced. Unlike confocal Raman micro-spectroscopy, also a non-invasive method, STRAFI-MRI is not limited to relatively thin depths (about 50 μm) [21]. 1D images were obtained from the resin and from CR, before and after being light-cured; in addition, 2D images were recorded from cured samples. Figure 6a shows typical 1D projections obtained from the resin after 10 s and 10 + 20 s irradiation periods; in order to favour the visualization of more mobile domains, hence with long T_2, only the last eight echoes in each echo train were used for profile reconstruction. In fact, because each data point in a profile is the result of the summation of the last eight echoes in an echo train, a less intense signal is obtained for more rigid domains because, in this case, the echo intensity decays faster. It must be noticed that, in these figures, the profiles are rotated of 90° and, consequently, the sample surfaces and the reference signals obtained from plastic discs, are shown on the left- and on the right-side of the plots, respectively. Glass from the containers does not contain hydrogen nuclei, nuclei that were observed in the present study; accordingly, no signal is displayed between the profiles of the plastic disc and the samples. Similar data were recorded from CR 50 wt.% filler loaded, which are displayed in Fig. 6b. The first general observations are the decrease in signal intensity and the narrowing of the profiles after a longer exposure to light. The latter effect is clearly associated with contractions during polymerization and hence overall volume reduction. Because cured systems exhibit extensively lower

magnetization, an estimate of the extent of the reaction, which must not be considered here as DC, could be directly drawn from magnetization measurements. A close examination of the profiles obtained after 10 s irradiation time shows that the highest intensity in the resin profile (indicated by an arrow in Fig. 6a) is from surface slices while, conversely, the profile recorded from CR shows the opposite trend. Hence, while the resin shows a higher extent of reaction at the bottom of the container, CR starts by curing near the light source and the profile reproduces the significant light intensity drop with distance. In other words, CR shows a depth of cure lower than unloaded resins, which present a depth of cure higher than the thickness of the samples observed here (about 4 mm). The light source-distance effect was already observed on homopolymerizations but then the intensity used for curing (1 mW/cm^2) was much less than in the present study [22]. These data demonstrate clearly that the O_2 inhibitor influence is the dominant effect that explains the behaviour of the unloaded resin. It may be also observed that the intensity of both profiles decrease after a second irradiation period of 20 s but the effect is much more pronounced for CR. Resins and composite resins shrink during polymerization, mainly because the monomeric units of the polymer are then located within covalent bond distance of each other, that is, closer to one another than they were in the original monomer state. Using 1D images it was possible to estimate VPC, which were about 3.00 and 0.35 % ± 0.11% for the unfilled resin and for CR (50 wt.% filler), respectively. These data agree well with DC (shown in Table 1): higher DC determined higher VPC.

Figure 6a' and b' show 2D images obtained from the resin and from CR, 50 wt.% filler loaded, after being light-irradiated over 10 s and 10 + 20 s, respectively. As for 1D images, for higher T_2 contrast, only eight last echoes in each echo train were used for image reconstruction and the images are also rotated of 90° and, consequently, sample surfaces are shown on the left-side of the images. The images are shown as isosurface contours of the threshold data, after thresholding at a selected grey-level. Hence, regions with same colour represent domains with similar mobility. The reference signal for the magnetization intensity is only visible on the right-side of the image recorded from CR (Fig. 6b') because was chosen a lower level to cut off the signal contribution. 2D images also revealed that the samples were not uniformly cured. In particular, the cured unfilled resin presents a strong oxygen inhibitor effect, which is more clearly depicted on the 2D image shown in Fig. 6a' than in the profile presented in Fig. 6a; a surface layer about 0.5 mm thick is observed in that image, showing the presence of highly mobile regions where the conversion appears to be low.

The amount of reacted monomer in the cured materials was determined by FTIR spectroscopy (resin/DC = 49.6 ± 0.9 mol% and composite 50 wt.% filler/DC = 32.0 ± 0.7 mol%) and the results explain the observation of highly mobile regions in STRAFI-MRI profiles and images recorded from resins and CR even after being irradiated over 10 + 20 s (Fig. 6). The decrease of DC with filler loading (Table 1) could be explained by the fact that the increase of filler content leads to a DC reduction at higher specimen depth due to a less extent of light penetration; Fig. 6b shows the occurrence of higher molecular mobility near the bottom of the cured CR. On the other hand, the cured unfilled resin presents a strong oxygen inhibitor effect which is visible in Fig. 6a and a'; this effect was not

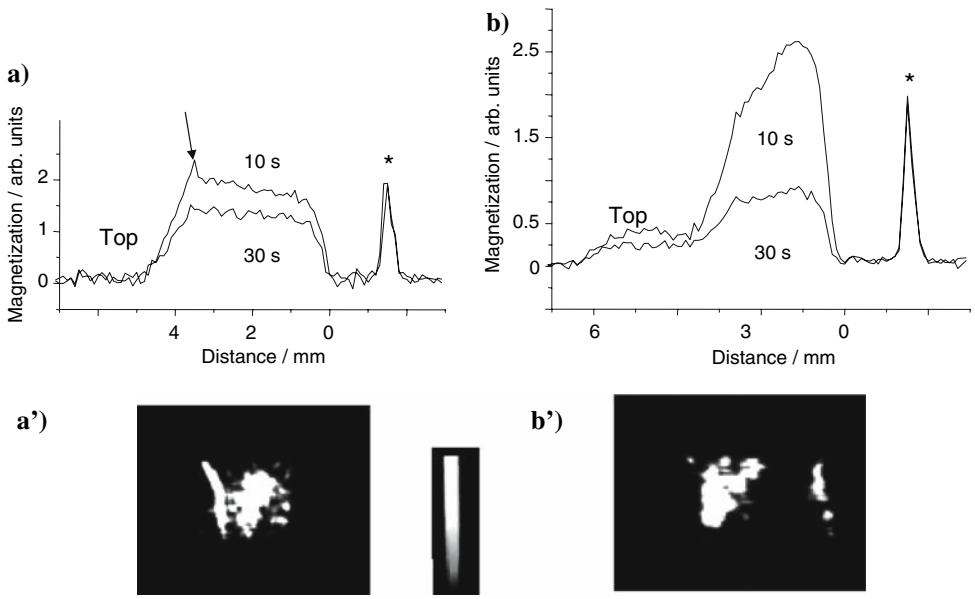

Fig. 6 STRAFI ^{1}H magnetization projections obtained from unfilled resin (**a**) and resin 50 wt.% filler loaded (**b**) after 10 s and 10 + 20 s irradiation times, using for the profile reconstruction only the last eight echoes in each echo train. Magnetizations were normalized using the signal shown on the right side (*), which is from a plastic disc. The sample surfaces (top) are on the left side. 2D STRAFI ^{1}H magnetization images obtained from specimens cured over: (**a'**) 10 s, unfilled resin and (**b'**) a total of 30 s, resin 50 wt.% filler loaded (resolution/pixel: 0.1 × 0.1 mm^2)

observed by 1D and 2D STRAFI-MRI images in CR and this is explained by a viscosity increase with filler loading, hence to lower solubility of molecular oxygen. Recently, it was shown that unsilanized silica has increased the viscosity of the resin; nevertheless, the increase of oxygen diffusivity, which has an opposite effect on DC, was suggested as an explanation for the lack of significant changes of DC in the inhibited region ($\sim$50 μm, 60 s with 400 mW/cm^2) with filler content for composites 30% and lower filler loadings [21]. Conversely, data presented here clearly shows an increase of DC near the surface with treated filler content and this may indicate that SIL reduces oxygen diffusivity in CR.

4 Conclusions

Evidence was provided for complete hydrolysis of the methoxyl groups during silanization of the particulate filler. Well resolved ^{1}H signals from αCH_2 to the silicon atoms in T^2 and T^3 units were obtained for the first time. While T^3 components appeared to be mostly from physically adsorbed treated filler particles, our results support the presence of silane-resin chemical interaction involving predominantly T^2 units. This interaction provides a route for photopolymerization inhibition, hence explaining the VPC decrease observed with filler loading. Photopolymerization of unfilled resins occurred faster near the bottom of the container; conversely, CR curing reaction was primarily observed in domains near the light-source, indicating a more important filler influence *versus* oxygen inhibitor role, as probed by the observed depth of cure effect. Overall, at higher loadings, the polymerization shrinkage was less but at the same time a DC decrease was observed. It was found, in particular, that resins and composite resins were strongly inhomogeneously cured after irradiation periods generally recommended for in vivo restorations. This effect, which was enhanced under low intensity of light, was more important for composite resins.

Acknowledgements This work was supported by the Portuguese Foundation for Science and Technology (Grant: PRAXIS/BD/20066/99 and SFRH/BPD/25112/2005 and Projects: POCTI/33193/99 and PDCT/55395/04). The authors wish to thank KERR (USA) for kindly providing the filler.

References

1. S. G. PEREIRA, R. OSORIO, M. TOLEDANO, and T. G. NUNES, *Dent. Mater.* **21** (2005) 823
2. S. G. PEREIRA, R. OSORIO, M. TOLEDANO, M. A. CABRERIZO-VILCHEZ, T. G. NUNES, and S. KALACHANDRA, *Dent. Mater.* **23** (2007) 1189
3. L. MUSANJE, and J. L. FERRACANE, *Biomaterials* **25** (2004) 4065
4. F. BAUER, H. ERNST, U. DECKER, M. FINDEISEN, H. J. GLASEL, and H. LANGGUTH et al., *Macromol. Chem. Phys.* **201** (2000) 2654
5. I. SIDERIDOU, V. TSERKIT, and G. PAPANASTASIOU, *Biomaterials* **24** (2003) 655
6. R. H. HALVORSON, R. L. ERICKSON, and C. L. DAVIDSON, *Dent. Mater.* **19** (2003) 327
7. M. ATAI, and D. C. WATTS, *Dent. Mater.* **22** (2006) 785
8. D. F. TAYLOR, S. KALACHANDRA, M. SANKARAPANDIAN, and J. E. MCGRATH, *Biomaterials* **19** (1998) 197
9. T. G. NUNES, R. PIRES, J. PERDIGÃO, A. AMORIM, and M. POLIDO, *Polymer* **42** (2001) 8051
10. T. G. NUNES, G. GUILLOT, S. G. PEREIRA, and R. PIRES, *J. Phys. D: Appl. Phys.* **35** (2002) 1251
11. S. G. PEREIRA, T. G. NUNES, and S. KALACHANDRA, *Biomaterials* **23** (2002) 3799
12. F. RUEGGEBERG, D. HASINGER, and C. FAIRHURST, *Dent. Mater.* **6** (1990) 241
13. P. MIRAU, and S. HEFFNER, *Macromolecules* **32** (1999) 4912
14. H. GLASEL, F. BAUER, H. ERNST, M. FINDEISEN, E. HARTMANN, H. LANGGUTH, and R. SCHUBERT, *Macromol. Chem. Phys.* **201** (2000) 2765
15. F. BAUER, H. ERNST, D. HIRSCH, S. NAUMOV, M. PELZING, V. SAUERLAND, and R. MEHNERT, *Macromol. Chem. Phys.* **205** (2004) 1587
16. F. HEATLEY, Y. PRATSITSILP, N. McHUGH D. C. WATTS, and H. DEVLIN, *Polymer* **36** (1995), 1859
17. SDBS Web: http://www.aist.go.jp/RIODB/SDBS/ (National Institute of Advanced Industrial Science and Technology), March 2006
18. E. PRETSCH, and A. ROBIEN, *Anal. Chim. Acta* **248** (1991) 82
19. D. R. MORGAN, S. KALACHANDRA, H. K. SHOBHA, N. GUNDUZ, and E. O. STEJSKAL, *Biomaterials* **21** (2000) 1897
20. R. SCHALLER, C. ARNOLD, and E. PRETSCH, *Anal. Chim. Acta* **312** (1995) 95
21. M. A. GAUTHIER, I. STANGEL, T. H. ELLIS, and X. X. ZHU, *J. Dent. Res.* **84** (2005) 725
22. S. G. PEREIRA, N. REIS, and T. G. NUNES, *Polymer* **46** (2005) 8034